Journal of
Synchrotron
Radiation

ISSN 0909-0495

Received 8 February 2005
Accepted 6 May 2005

On the refinement of time-resolved diffraction data: comparison of the random-distribution and cluster-formation models and analysis of the light-induced increase in the atomic displacement parameters

Ivan I. Vorontsov and Philip Coppens*

Department of Chemistry, State University of New York at Buffalo, NY 14260, USA.
E-mail: coppens@buffalo.edu

Expressions for the random-distribution and cluster-formation models for light-induced changes in crystals studied by time-resolved diffraction are presented. The two models can be distinguished on the basis of differences in the predicted intensities. The light-induced increase in the atomic displacement parameters is analyzed with both simulated and experimental data sets.

Keywords: time-resolved diffraction; pump–probe technique; random-distribution model; cluster-formation model.

1. Introduction

Time-resolved (TR) diffraction studies using pump–probe techniques at synchrotron sources, in which the crystals are excited with a laser pulse immediately prior to a probing X-ray pulse, are opening a new area of importance in a broad range of physical sciences. The effect of laser light on molecular crystals may involve dramatic and often macroscopic irreversible changes such as surface melting and reorganization (Larsson *et al.*, 1998; Reis *et al.*, 2001), solid-state chemical reactions (Busse *et al.*, 2002; Kawano *et al.*, 2003) and phase transitions (Nasu, 1997; Larsson *et al.*, 2004; Collet *et al.*, 2003; Guérin *et al.*, 2004). Some of these phenomena cause a drastic change in the diffraction pattern because of the growth of domains of a new crystalline phase. As a result the diffraction patterns of the initial and photo-induced phases are superimposed, with Bragg spots coinciding only if the change in cell dimensions is minimal. On the other hand, in many chemical conversions, such as light-induced linkage isomerization (Fomitchev *et al.*, 2000; Kovalevsky *et al.*, 2002, 2003) and reversible photoexcitation (Coppens, 2003; Techert & Zachariasse, 2004; Kim *et al.*, 2002; Armaroli, 2001; Coppens *et al.*, 2004*a*; Coppens, Gerlits *et al.*, 2004), a random distribution of the generated species occurs with preservation of the original crystallographic symmetry. It is conceivable, however, that the distribution of the photoexcited species would not be random, but that cluster formation occurs. The local disturbance of the packing owing to excitation of a first molecule could, for example, sensitize adjacent molecules if the disturbance is sufficiently large. If the size of such clusters is similar or larger than the coherence length of the X-rays in the crystal, the scattering formalism will be affected.

The current paper deals with the situation in which all, or the large majority, of the 'dark' and 'light-on' diffraction peaks are superimposed. As the experiments are most sensitive when a *change* in the diffraction pattern is analyzed, the standard structure refinement algorithms which are based on minimization of an error function defined in terms of the structure factors F or F^2 are less suitable in time-resolved data analysis and new approaches must be developed. We describe here the generalization of earlier equations (Ozawa *et al.*, 1998), incorporated in the program *LASER* by Ozawa (Ozawa *et al.*, 1998) and by Pillet (Kim *et al.*, 2002), to include both the random-distribution and cluster-formation models and the possibility of distinguishing between the two models. The relative effect of the photo-induced disorder in the random-distribution model and the temperature increase during illumination are also discussed.

2. Response ratios as observables in the refinement procedure

In the TR experiment data are collected both during laser-on and under dark conditions. The time resolution is limited by the width of the exciting laser pulse, the width of the probing X-ray pulse and the ability of the X-ray shutter to select one or more X-ray pulses from the stream provided by the light source. When the transient state rapidly reverts to the ground state a stroboscopic method can be used in which the exciting laser pulses are repeated thousands of times per second as the frame of data is being collected and the X-ray probe pulses are synchronized with the excitations (Kim *et al.*, 2002; Coppens *et al.*, 2005). The response ratio $\eta(hkl)$ is defined as the fractional

change in the intensity of a reflection during exposure relative to the dark measurement,

$$\eta(hkl) = \frac{\left[I_{\rm on}(hkl) - I_{\rm off}(hkl)\right]}{I_{\rm off}(hkl)} = \frac{\left[F^2_{\rm on}(hkl) - F^2_{\rm off}(hkl)\right]}{F^2_{\rm off}(hkl)}, \quad (1)$$

where I and $F^2(hkl)$ are the intensity and squared structure factor, respectively, and the subscripts 'on' and 'off' refer to the values during and without laser exposure, respectively.

The corresponding error function to be minimized in the least-squares procedure becomes

$$S = \sum_i w_i \left(\eta_i^{\rm obs} - \eta_i^{\rm calc}\right)^2, \quad (2)$$

where $\eta^{\rm obs}$ and $\eta^{\rm calc}$ are the observed and calculated response ratios, respectively, and the weights are defined by $w_i = 1/\sigma_i^2(\eta^{\rm obs})$.

The advantages of using the response ratios rather than the F^2 or $|F|$ values in the least-squares refinement is that their values are relatively independent of crystal decay during the intense laser exposure. Long-term instabilities in the intensity and position of the X-ray beam are eliminated because of the strategy of data collection in which light-off frames are immediately collected after the light-on measurement. In addition, use of the response ratios facilitates combining data from different sample crystals, which is generally required because of the limited life of the crystals in the laser beam.

As the minimization involves the response ratios rather than the structure factors, the merit factors for judging the convergence of the refinement are

$$R = \sum_i |\eta_i^{\rm obs} - \eta_i^{\rm calc}| \Big/ \sum_i |\eta_i^{\rm obs}|, \quad (3)$$

$$wR = \left[\sum_i w_i |\eta_i^{\rm obs} - \eta_i^{\rm calc}|^2\right]^{1/2} \Big/ \left[\sum_i w_i |\eta_i^{\rm obs}|^2\right]^{1/2}, \quad (4)$$

$$\text{Gof} = \left[\sum_i w_i |\eta_i^{\rm obs} - \eta_i^{\rm calc}|^2\right]^{1/2} \Big/ (n-m)^{1/2}, \quad (5)$$

where the index i indicates the summation over all observations, and n and m represent the number of observations and variables, respectively.

3. Least-squares variables

As the refinement is on the changes in the light-off structure a reliable dark structure is an essential reference in the analysis. Proper care must be taken to account for changes in the unit-cell parameters, which may be due to temperature increase of the sample in the laser beam or to the change in molecular shape on excitation. The latter effect is negligible when conversion percentages are small ($\sim$10% or less), as is the case in the time-resolved studies performed so far, but can be considerable in studies of light-induced metastable states (see, for example, Fomitchev *et al.*, 1998). The possibility of a temperature increase in the sample is accounted for in the data analysis by application of a scale factor k_B to the displacement parameters of every atom, *i.e.* $U_{\rm on}(ij) = k_B U_{\rm off}(ij)$, where $U_{\rm on}(ij)$ and $U_{\rm off}(ij)$ are displacement parameters of the light-on and light-off structures.

The initial value of k_B is obtained from a modified Wilson plot in which $\ln(I_{\rm on}/I_{\rm off})$ is plotted *versus* $(\sin\theta/\lambda)^2$, as discussed further below. The slope of the plot provides an estimate of $2\Delta B$ where ΔB equals $B_{\rm overall,\,off} - B_{\rm overall,\,on}$. The initial estimate for k_B then follows from

$$k_B = 1 + |\Delta B_{\rm WP}|/(8\pi^2 U_{\rm ave}), \quad (6)$$

in which $U_{\rm ave}$ is the ground-state isotropic displacement parameter typical for the heavier atoms, which dominate the high-order scattering.

Other variables include the excited-state population, positional parameters of the excited-state atoms, and rotations and translations of rigid bodies in the excited species as well as rigid-body translational and rotational motions of the unconverted molecules. Although excited-state temperature parameters of the individual atoms can be refined, owing to the typically small excited-state population and often limited data it is generally necessary to use the ground-state displacement parameters modified by k_B, as described above.

4. Cluster-formation formalism (CF) *versus* random distribution (RD)

If the excited species are randomly distributed in the crystal, the coherent diffraction pattern reflects the space-averaged structure, whereas the effect of the photo-induced disorder is reflected in the diffuse scattering pattern. A crucial distinction with disorder as encountered frequently in crystal structure analysis is that in the photocrystallographic case detailed information is available from the dark experiment on one of the components of the disordered crystal. If p is the population of the converted species, the RD structure factor expression for the coherent Bragg intensities is given by

$$\vec{F}_{\rm on} = (1-p)\vec{F}_{\rm ground} + p\vec{F}_{\rm excited}, \quad (7a)$$

or, if a possible modification of the ground-state structure by the intruding excited species is taken into account,

$$\vec{F}_{\rm on} = (1-p)\vec{F}_{\rm ground,on} + p\vec{F}_{\rm excited,on}, \quad (7b)$$

in which the putative difference between the pre-exposure and during-exposure ground-state component is accounted for. This algorithm has been successfully applied in a series of studies of crystals containing metastable and light-induced excited-state species, including cases with a conversion percentage close to 50% (Coppens *et al.*, 2004*a*; Coppens, Gerlits *et al.*, 2004; Fomitchev *et al.*, 2000; Kim *et al.*, 2002; Kovalevsky *et al.*, 2002, 2003). It implies the absence of extra spots in the diffraction pattern.

The CF model assumes that the excited molecules cluster to form domains of a new phase with dimensions larger than the X-ray coherence length. This is similar to a photo-induced phase transition, which may lead to the occurrence of a second diffraction pattern or, if the two phases are alike, to a superposition of the reflections of the two phases. The latter case is

encountered in the neutral to ionic phase transformation of TTF-chloranil (Collet *et al.*, 2003; Guérin *et al.*, 2004) in which, apart from a number of photo-induced $(0k0)$ reflections resulting from the loss of the 2_1 axis of the monoclinic space group, the diffraction patterns are fully superimposed. The photochemical process has a high quantum yield as each photon initiates a chain formation of the molecular ion pairs.

The CF scattering formalism appropriate to this case is

$$F_{\rm on}^2 = (1-p)F_{\rm ground}^2 + pF_{\rm excited}^2. \quad (8)$$

When expression (7) is squared, the difference between the two cases becomes evident. For the RD model,

$$F_{\rm on}^2 = (1-p)^2F_{\rm ground}^2 + p^2F_{\rm excited}^2 + 2p(1-p)\vec{F}_{\rm ground}\vec{F}_{\rm excited}. \quad (9)$$

Substitution of $F_{\rm excited} = F_{\rm ground} + \Delta$, where Δ may be positive or negative, gives, in the centrosymmetric case,

$$\text{CF}: \quad F_{\rm on}^2 = F_{\rm ground}^2 + 2p\Delta F_{\rm ground} + p\Delta^2 \quad (10)$$

and

$$\text{RD}: \quad F_{\rm on}^2 = F_{\rm ground}^2 + 2p\Delta F_{\rm ground} + p^2\Delta^2. \quad (11)$$

Thus,

$$F_{\rm on,MP}^2 - F_{\rm on,RD}^2 = (p-p^2)\Delta^2. \quad (12)$$

When $p = 1$ (or $\Delta = 0$) the two models are identical as expected. Since p is always less than 1, for a given distortion $F_{\rm on,RD}^2$ is always smaller than $F_{\rm on,CF}^2$. For a given reflection the difference is maximal for $p = 0.5$, and decreases symmetrically on each side of this value. The prediction that $F_{\rm on,CF}^2$ is always larger is born out by a model calculation performed to simulate the TR diffraction experiment on $\{[3,5\text{-}(CF_3)_2\text{pyrazolate}]Cu\}_3$, in which a large shift of the Cu atoms was observed leading to intermolecular bond formation (Vorontsov *et al.*, 2005). The results of the simulation (Fig. 1), with an assumed excited-state population of 12%, indicate that for a reasonable conversion percentage the two models lead to quite different intensities and thus should be easily distinguishable.

The Wilson plots based on the intensities according to the two models (Fig. 2), calculated using expressions (7) and (8), noticeably differ in that the RD model gives a negative intercept with the y axis, whereas the value at $(\sin\theta/\lambda)^2 = 0$ tends to be positive for the CF model data. The negative intercept can be understood as resulting from the photo-induced reduction of the average intensity in the RD situation.

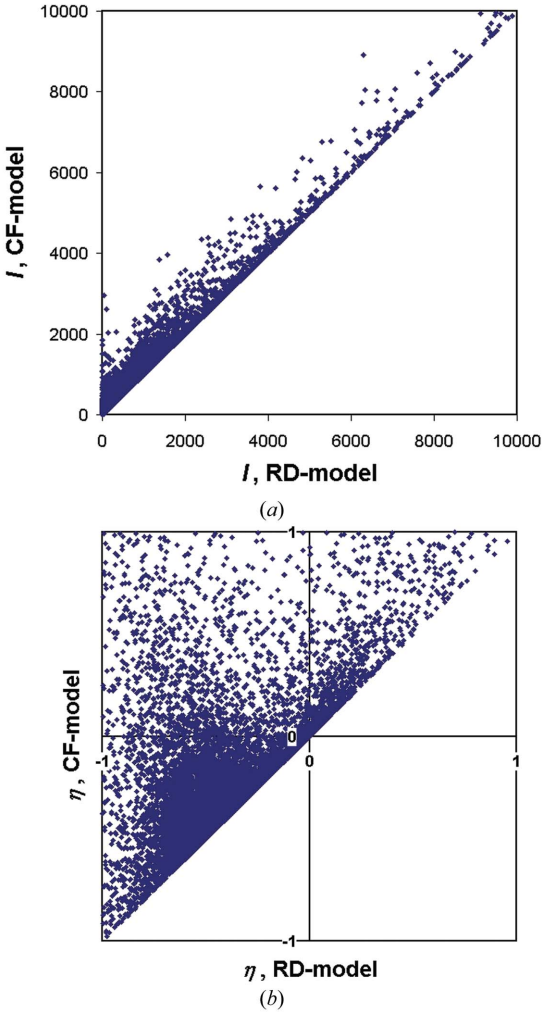

Figure 1
Correlation plots of the intensity effect from the cluster formation (CF) model *versus* the random distribution (RD) model (*a*) on intensities, (*b*) on the response ratios. Simulated data on $\{[3,5\text{-}(CF_3)_2\text{pyrazolate}]Cu\}_3$, 12% excited-state population.

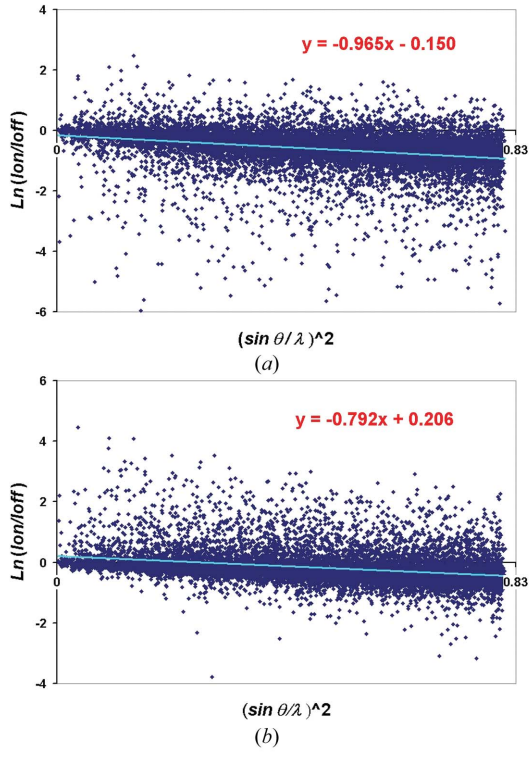

Figure 2
Wilson plots for RD (*a*) and CF (*b*) simulations of the TR diffraction experiment on $\{[3,5\text{-}(CF_3)_2\text{pyrazolate}]Cu\}_3$. Excited-state population assumed as 12%, $k_B = 1.87$, including 12240 and 12239 reflections with $\eta > 2\sigma(\eta)$ for the RD and CF models, respectively.

The positive intercept found in the simulation for the CF model is less easily rationalized and may be specific for the case under examination. A criterion for rapid distinction between the two models, applicable as the experiment proceeds, may be based on this observation. An experimental example is discussed below.

5. Expression for the derivatives of η in the RD and CF models

The intrinsic difference between the two models is evident in the expressions for the derivatives to be used in the least-squares procedure. The derivatives of the response ratios for the parameters other than p are as follows. For the RD model,

$$\frac{\partial \eta}{\partial u} = \frac{\partial}{\partial u}\left(\frac{F_{\rm on}^2}{F_{\rm off}^2}\right) = 2\left(\frac{1}{F_{\rm off}^2}\right)\left(A_{\rm on}\frac{\partial A_{\rm on}}{\partial u} + B_{\rm on}\frac{\partial B_{\rm on}}{\partial u}\right) \quad (13)$$

in which $A_{\rm on}$ and $B_{\rm on}$ include the population p, and for the CF model,

$$\frac{\partial \eta}{\partial u} = 2\left(\frac{1}{F_{\rm off}^2}\right)\left[(1-p)\left(A'_{\rm on,gr}\frac{\partial A'_{\rm on,gr}}{\partial u} + B'_{\rm on,gr}\frac{\partial B'_{\rm on,gr}}{\partial u}\right) + p\left(A'_{\rm on,exc}\frac{\partial A'_{\rm on,exc}}{\partial u} + B'_{\rm on,exc}\frac{\partial B'_{\rm on,exc}}{\partial u}\right)\right] \quad (14)$$

where $A'_{\rm on}$ and $B'_{\rm on}$ of the homogeneous phases are exclusive of the population parameters. The corresponding derivatives for population are

$$\frac{\partial \eta}{\partial p} = 2\left(\frac{1}{F_{\rm off}^2}\right)\left[A_{\rm on}\left(A_{\rm on}^{\rm excited} - A_{\rm on}^{\rm ground}\right) + B_{\rm on}\left(B_{\rm on}^{\rm excited} - B_{\rm on}^{\rm ground}\right)\right] \quad (15)$$

for the RD model and

$$\frac{\partial \eta}{\partial p} = 2\left(\frac{1}{F_{\rm off}^2}\right)\left(F_{\rm exc}^2 - F_{\rm gr}^2\right) \quad (16)$$

for the CF model.

6. Simulated analysis of the effect of temperature *versus* the photo-induced disorder

It is well known that disorder in a crystal leads to a decrease in the intensity of the coherent diffraction peaks. Since Δ/F will be larger for the high-order reflections, which are more sensitive to the detail of the distribution of the scattering electrons, the effect of disorder is equivalent to an apparent increase in the atomic temperature factors, which are indeed atomic displacement parameters (ADPs). The Wilson plots of $\ln(I_{\rm on}/I_{\rm off})$ *versus* $(\sin\theta/\lambda)^2$ (Figs. 2 and 5) thus reflect the effect of the temperature increase during the on-period as well as the photo-induced disorder in the crystal.

To examine the relative contribution of the two effects in a real case, a simulated data set was generated for a crystal of the photosensitizer dye Cu(dmp)(dppe)PF_6 [dmp = 2,9-dimethylphenanthroline, dppe = 1,2-bis(diphenylphosphino)-ethane] which has been the subject of a TR study (Coppens *et al.*, 2004*b*). It crystallizes with two molecules in the monoclinic asymmetric unit (Z = 8, $P2_1/c$). Positional and temperature factors were taken from the ground-state crystal structure. To simulate the effect of light, the unit-cell volume was increased by 40 Å^3 (corresponding to 0.6% of the unit-cell volume, which according to the temperature dependence of the cell dimensions would be an increase of the sample temperature of about 50 K) with an adjustment of the fractional coordinates to keep the intermolecular distances invariant, and a small shift and a rotation (less that 1°) were applied to the ground-state cations and PF_6 counter-ions. In accordance with the experimental result, the position and orientation of the ligands attached to the Cu were changed by applying flattening (*i.e.* a change from 90° of the angle between the P—Cu—P and N—Cu—N planes) and rocking distortions (defined as the angle between Cu—$X_{\rm P}$ and Cu—$X_{\rm N}$ vectors, where $X_{\rm P}$ and $X_{\rm N}$ are the centers of the P—P and N—N vectors) (Fig. 3), a shortening of the Cu—N, and lengthening of the Cu—P distances. In addition, ~0.3 Å rigid-body shifts were applied to the excited-state molecules. The initial k_B factors in the simulation and the values derived from the Wilson plots are presented in Table 1.

Table 1
Overall displacement parameters from Wilson plots of simulated data sets.

Model	Initial k_B	$2\Delta B$ from Wilson plot (Å^2)	k_B from $2\Delta B$
ΔT + disorder	1.70	1.28	1.74
ΔT only	1.70	1.02	1.58
Disorder only	–	0.32	1.18

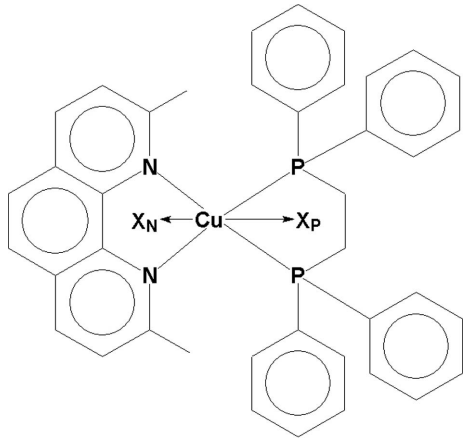

Figure 3
Definition of the distortion angles of the CuN_2P_2 group of Cu(dmp)-(dppe)PF_6.

The values in the 'ΔT only' row of Table 1 indicate that the Wilson plot underestimates the pure temperature effect, whereas the entries in the first and third rows confirm that the photo-induced disorder contributes to the temperature scale factor derived from the Wilson plot. The same conclusion is reached with the simulated data for {[3,5-$(CF_3)_2$pyrazolate]Cu}$_3$, for which the Wilson plots (Fig. 2) give k_B estimates of 2.22 and 2.01 for the RD and CF models, respectively,

whereas the data were generated with $k_B = 1.87$. Nevertheless, the k_B values from the statistical plots are clearly appropriate as starting points in the least-squares refinement. The contribution of the photo-induced disorder to the change in atomic displacement parameters as deduced from the Wilson plots is relatively small. When the photo-induced disorder is accounted for in the scattering model the artificial increase will disappear, as confirmed by subsequent refinement of the simulated data sets.

7. An experimental example

Time-resolved diffraction experiments on crystals of trimeric {[3,5-$(CF_3)_2$pyrazolate]Cu}$_3$ (Fig. 4) were performed at the 15-ID beamline at the Advanced Photon Source (Vorontsov *et al.*, 2005). The crystals are strongly phosphorescent when exposed to light in the UV region (Dias *et al.*, 2005). On illumination with a 366 nm laser beam at 17 K, a phosphorescent lifetime of 53 µs is observed.

The Wilson plot of the data set with 7187 response ratios >2σ, on which the analysis was based, had a slope of −0.665 (Fig. 5), from which, with a value of $U_{\rm overall}$ of 0.005 Å^2, a $k_{\rm B}$ factor equal to 1.87 was derived. The subsequent refinement based on the RD formalism led to a temperature scale factor value of 2.055 (8). The structure refinement showed a large contraction of one of the intermolecular Cu—Cu distances from 4.018 (1) Å to 3.46 (1) Å, leading to the formation of a highly phosphorescent excimer (excited dimer). Since the photon-triggered process was clearly intermolecular, the CF model is a possible alternative. However, the Wilson plot shows an intercept of the least-squares line with the *y* axis at a negative *y* value, which according to the simulations described above indicates that the RD model is appropriate. This conclusion is confirmed by the refinement. While convergence at $R(\eta) = 0.32$ was reached in seven cycles with the RD model, no convergence could be achieved based on the CF algorithm, which gave merit factors oscillating in the 0.44–0.57 range.

It should be noted here that *R* factors from response ratio refinements cannot be compared with those used in a conventional structure analysis in which intensities are measured within an accuracy of a few percent, a precision not attainable for the response ratios, few of which exceed ten standard deviations in a typical experiment.

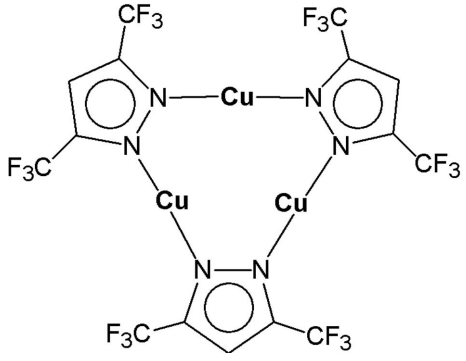

Figure 4
Diagram of the {[3,5-$(CF_3)_2$pyrazolate]Cu}$_3$ trimer.

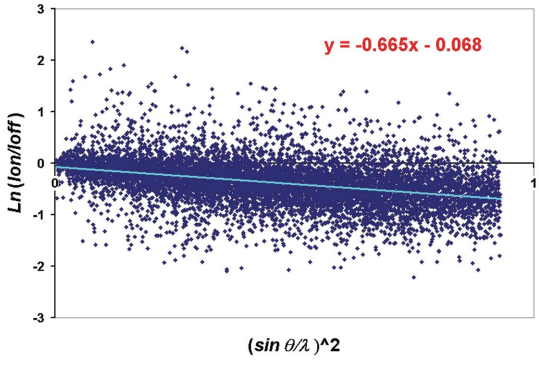

Figure 5
Experimental Wilson plot for a {[3,5-$(CF_3)_2$pyrazolate]Cu}$_3$ TR data set. The vertical size of the spots corresponds to 1.5 times the average standard deviation.

8. Conclusions

We conclude that the two physical models examined in this study lead to quite different intensity predictions and can be distinguished on this basis. The statistical Wilson plots based on the ratios of the light-on and light-off intensities can be used to provide an initial indication as to which model is appropriate. The Wilson plots are affected by the disorder present if the excited species are randomly distributed in the crystal, but nevertheless provide an appropriate estimate for the starting value of the temperature scale factor which is needed in the subsequent refinement procedure.

Support of this work by the US Department of Energy through grant DE-FG02-02ER15372 and by the National Science Foundation (CHE0236317) is gratefully acknowledged.

References

Armaroli, N. (2001). *Chem. Soc. Rev.* **30**, 113–124.
Busse, G., Tschentscher, T., Plech, A., Wulff, M., Frederichs, B. & Techert, S. (2002). *Faraday Discuss.* **122**, 105–117.
Collet, E., Lemee-Cailleau, M.-H., Buron-Le Cointe, M., Cailleau, H., Wulff, M., Luty, T., Koshihara, Sh.-Ya., Meyer, M., Toupet, L., Rabiller, Ph. & Techert, S. (2003). *Science*, **300**, 612–615.
Coppens, P. (2003). *Chem. Commun.* **12**, 1317–1318.
Coppens, P., Gerlits, O., Vorontsov, I. I., Kovalevsky, A. Y., Chen, Y.-S., Graber, T. & Novozhilova, I. V. (2004). *Chem. Commun.* pp. 2144–2145.
Coppens, P., Vorontsov, I. I., Graber, T., Gembicky, M. & Kovalevsky, A. Yu. (2005). *Acta Cryst.* A**61**, 162–172.
Coppens, P., Vorontsov, I. I., Graber, T., Kovalevsky, A. Yu., Chen, Y.-S., Wu, G., Gembicky, M. & Novozhilova, I. V. (2004*a*). *J. Am. Chem. Soc.* **126**, 5980–5981.
Coppens, P., Vorontsov, I. I., Graber, T., Kovalevsky, A. Yu., Chen, Y.-S., Wu, G., Gembicky, M. & Novozhilova, I. V. (2004*b*). *J. Am. Chem. Soc.* **126**, 5980–5981.
Dias, H. V. R., Diyabalanga, H. V. K., Eldabaja, M. G., Elbjeirama, O., Rawashdeh-Omary, M. A. & Omary, M. A. (2005). Submitted.
Fomitchev, D. V., Furlani, T. R. & Coppens, P. (1998). *Inorg. Chem.* **37**, 1519–1526.

Fomitchev, D. V., Novozhilova, I. & Coppens, P. (2000). *Tetrahedron*, **56**, 6813–6820.
Guérin, L., Collet, E., Lemée-Cailleau, M.-H., Buron-Le Cointe, M., Cailleau, H., Plech, A., Wulff, M., Koshihara, S.-Y. & Luty, T. (2004). *Chem. Phys.* **299**, 163–170.
Kawano, M., Takayama, T., Uekusa, H., Ohashi, Y., Ozawa, Y., Matsubara, K., Imabayashi, H., Mitsumi, M. & Toriumi, K. (2003). *Chem. Lett.* **32**, 922–923.
Kim, C. D., Pillet, S., Wu, G., Fullagar, W. K. & Coppens, P. (2002). *Acta Cryst.* A**58**, 133–137.
Kovalevsky, A. Yu., Bagley, K. A., Cole, J. M. & Coppens, P. (2003). *Inorg. Chem.* **42**, 140–147.
Kovalevsky, A. Yu., Bagley, K. A. & Coppens, P. (2002). *J. Am. Chem. Soc.* **124**, 9241–9248.
Larsson, J., Heimann, P. A., Lindenberg, A. M., Schuck, P. J., Bucksbaum, P. H., Lee, R. W., Padmore, H. A., Wark, J. S. & Falcone, R. W. (1998). *Appl. Phys. A*, **66**, 587–591.
Larsson, J., Sondhauss, P., Synnergren, O., Harbst, M., Heimann, P. A., Lindenberg, A. M. & Wark, J. S. (2004). *Chem. Phys.* **299**, 157–161.
Nasu, K. (1997). Editor. *Relaxations of Excited States and Photo-Induced Structural Phase Transitions, Springer Series in Solid-State Sciences*, Vol. 124. Berlin: Springer.
Ozawa, Y., Pressprich, M. R. & Coppens, P. (1998). *J. Appl. Cryst.* **31**, 128–135.
Reis, D. A., DeCamp, M. F., Bucksbaum, P. H., Clarke, R., Dufresne, E., Hertlein, M., Merlin, R., Falcone, R., Kapteyn, H., Murnane, M. M., Larsson, J., Missalla, T. & Wark, J. S. (2001). *Phys. Rev. Lett.* **86**, 3072–3075.
Techert, S. & Zachariasse, K. A. (2004). *J. Am. Chem. Soc.* **126**, 5593–5600.
Vorontsov, I. I., Kovalevsky, A. Yu., Chen, Y.-S., Graber, T., Novozhilova, I. V., Omary, M. A. & Coppens, P. (2005). *Phys. Rev. Lett.* **94**. In the press.